

Positioning Method for an AUV in Arctic Seawater Based on Polarization

Bo Tang[✉], Member, IEEE, and Qiang Chen[✉], Senior Member, IEEE

Abstract—In this letter, a positioning method for an autonomous underwater vehicle (AUV) in the Arctic that uses an electromagnetic field is studied. The method uses the direction-of-arrival (DOA) triangulation based on the polarization of the near field of three positioning nodes. The positioning nodes each transmit a monochromatic wave with a different frequency. The AUV can obtain the polarized field, and then estimate its position through a comparison of the different components of the field. The positioning error caused by the measurement error of the different components of the field has been analyzed, and numerical simulations are in an agreement with the analysis. The positioning error caused by the fluctuation of the sea surface has also been analyzed. The results show that triangulation with a polarization-based DOA can be used for the positioning of an AUV in the Arctic seawater.

Index Terms—Autonomous underwater vehicle (AUV), direction-of-arrival (DOA), positioning, underwater.

I. INTRODUCTION

THE analysis and detection of electromagnetic fields in seawater have been researched for many years [1]–[4]. The radiation of a dipole in a dissipative media was studied by King [5]. The current distribution along the dipole and the impedance of the dipole were given in [5] and [6]. For better radiation efficiency, an insulated linear antenna was used [7], and the current distribution and impedance of the insulated linear antenna were analyzed using a transmission line theory [7]–[9]. A model of the stratified media was used to account for the air above the sea surface [10], [11]. An electromagnetic propagation is difficult to be detected due to attenuation in the seawater. At a low frequency, the seawater acts as a conduction material, in which the conduction current is far greater than the displacement current. The attenuation is approximately 55 dB through one wavelength in seawater at a low frequency [12]. Therefore, a line-of-sight channel is impractical for signal transmission in seawater. For practical communication between two dipoles immersed in seawater, the main path of communication is through the air above the sea surface [13]. For this reason, a horizontal

linear antenna is used to reduce path loss. The radiation field of a horizontal antenna has been studied in [14] and [15]. The power received by a sheath-covered antenna in seawater was studied based on a two-port equivalent circuit [16]. In addition to these analytical studies, experimental results were also presented in other studies [17]–[19]. Based on these works, the application of the electromagnetic field in seawater has been promoted in recent years.

A new application of the electromagnetic field in seawater is to position an autonomous underwater vehicle (AUV) under the polar ice cap using the horizontal sheath-covered electric dipole [20]. The main difficulty in this type of application comes from the low frequency of the transmitted signal. The low frequency leads to poor time and range resolutions and, thus, a poor accuracy in positioning. Hence, it is difficult to use the time-of-arrival method. Therefore, the direction-of-arrival (DOA) method is preferred. For DOA, the problem encountered in seawater is how to decouple range, azimuth, and depth. To deal with this problem, triangulation with polarization-based DOA using horizontal electric dipoles is studied in this letter.

A similar decoupling problem on range and azimuth is in the magnetoquasistatic-based positioning method above ground [21], [22]. The transmitter uses two electrically small coils that are orthogonal to each other, and so does the receiver. For the magnetoquasistatic-based positioning methods, there are differences between aboveground positioning and underwater positioning. First, the loop antennas need to be designed suitable for an underwater application. For example, seawater resistance is an issue to consider for an AUV that moves a long way. To deal with this, the loop antenna can be placed within the AUV fuselage if the fuselage is made of dielectric material. Second, the magnetoquasistatic-based positioning method uses the field strength to determine the distance; however, the field strength in seawater is extremely sensitive to the minor variation of the depth [17]. Therefore, the ranging error induced by the depth variation need to be considered. To avoid using the field strength in positioning, we adopt the triangulation based on DOA.

II. POSITIONING METHOD BASED ON POLARIZATION

A. DOA Based on a Polarized Electric Field

The horizontal dipoles are immersed in the seawater as the transmitting and receiving antennas. The positioning node has one dipole for transmitting; the AUV has two cross dipoles in horizontal plane for receiving the polarization components of the field. It is a 1×2 configuration. It is equivalent to a

Manuscript received October 22, 2018; revised November 28, 2018; accepted November 28, 2018. Date of publication December 5, 2018; date of current version January 3, 2019. This work was supported in part by the National Natural Science Foundation of China under Grant 61471041, and in part by the Fundamental Research Funds for the Central Universities under Grant FRF-TP-15-028A3.

B. Tang is with the School of Computer and Communication Engineering, University of Science and Technology Beijing, Beijing 10083, China (e-mail: tangbohr@hotmail.com).

Q. Chen is with the Graduate School of Engineering, Tohoku University, Sendai 980-8579, Japan (e-mail: chenq@ecei.tohoku.ac.jp).

Digital Object Identifier 10.1109/LAWP.2018.2885068

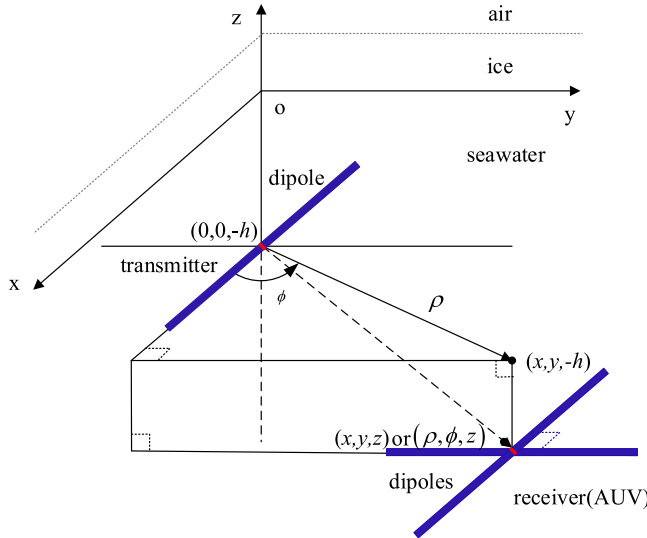


Fig. 1. Coordinate systems.

2×1 configuration. For convenience, the former is analyzed here. The coordinate systems are shown in Fig. 1. A rectangular coordinate system (x, y, z) and its corresponding cylindrical coordinate system (ρ, ϕ, z) are used simultaneously. The surface of the seawater is located in the xy plane. The ice layer and the air are above the xy plane. The center of the horizontal transmitting dipole is immersed at the position $(0, 0, -h)$ ($h > 0$) in the rectangular coordinate system such that the transmitting dipole is located h meters below the surface of the seawater. The orientation of the transmitting dipole is aligned with x -direction. The receiver is located at (x, y, z) in the rectangular coordinate system or (ρ, ϕ, z) in the corresponding cylindrical coordinate system. The orientations of the receiving dipoles are aligned with x -direction and y -direction, respectively. Only the near field is considered in this letter because of severe attenuation. The depth of the AUV can be obtained using a depth gauge. Therefore, the positioning can be simplified as a two-dimensional positioning problem.

When $\rho \gg h$, according to [14] and [15], the near field can be expressed as

$$E_x \cong \frac{Ids}{2\pi\sigma\rho^3} e^{\gamma(h-z)} (1 - 3\sin^2\phi) \quad (1)$$

$$E_y \cong \frac{Ids}{2\pi\sigma\rho^3} e^{\gamma(h-z)} (3\sin\phi\cos\phi) \quad (2)$$

where $\gamma = -\sqrt{\frac{\omega\mu_0\sigma}{2}}(1+j)$, σ is the conductivity of the seawater, I is the current on the dipole, and ds is the length of the dipole. For 10 kHz, (1) and (2) hold for $8.92 \text{ m} < \rho < 957 \text{ m}$ [14]. That is, the positioning method is valid only in this range for 10 kHz.

Although expressions (1) and (2) are originally for a two-layered stratified media with seawater and air in [14] and [15], they can also be used to approximate a three-layered stratified media with seawater, sea ice, and air because the wavenumbers both in sea ice and in air are much smaller than the wavenumber in seawater.

The receiver can detect the polarized field expressed in (1) and (2). Similarly to [21], let

$$\chi = \frac{E_x^2}{E_x^2 + E_y^2}. \quad (3)$$

By substituting (1) and (2) into (3), it can be obtained that

$$\chi = \frac{(1 - 3\sin^2\phi)^2}{(1 - 3\sin^2\phi)^2 + (3\sin\phi\cos\phi)^2}. \quad (4)$$

Therefore, ϕ satisfies the following equation:

$$9\sin^4\phi - (6 + 3\chi)\sin^2\phi + (1 - \chi) = 0. \quad (5)$$

The solution is

$$\sin\phi = \pm \sqrt{\frac{2 + \chi \pm \sqrt{\chi^2 + 8\chi}}{6}}. \quad (6)$$

The solution is not unique; therefore, there are some false solutions in (6) that must be eliminated. In (6), the solution of the azimuthal angle corresponds to four straight lines passing through the transmitting dipole or the positioning node.

B. Elimination of the False Solutions for the Azimuthal Angle

The measurement data can be used to determine whether E_x or E_y are in-phase or out-of-phase and can be used to eliminate some of the false solutions for the azimuthal angle. The four possible straight lines through the positioning node can be reduced to two possible straight lines.

Let

$$\alpha = \arcsin \sqrt{\frac{2 + \chi - \sqrt{\chi^2 + 8\chi}}{6}} \quad (7)$$

$$\beta = \arcsin \sqrt{\frac{2 + \chi + \sqrt{\chi^2 + 8\chi}}{6}}. \quad (8)$$

When E_x and E_y are in-phase, that is, $(1 - 3\sin^2\phi)\sin\phi\cos\phi > 0$, ϕ is in the range of $0 < \phi < \arcsin(1/3)$ and $\pi < \phi < \pi + \arcsin(1/3)$, or in the range of $\pi/2 < \phi < \pi - \arcsin(1/3)$ and $3\pi/2 < \phi < 2\pi - \arcsin(1/3)$. Therefore, the solutions are either $\phi = \alpha$ and $\phi = \alpha + \pi$ (first straight line through the positioning node) or $\phi = \pi - \beta$ and $\phi = 2\pi - \beta$ (second straight line through the positioning node).

When E_x and E_y are out-of-phase, that is, $(1 - 3\sin^2\phi)\sin\phi\cos\phi < 0$, ϕ is in the range of $\pi - \arcsin(1/3) < \phi < \pi$ and $2\pi - \arcsin(1/3) < \phi < 2\pi$ or in the range of $\arcsin(1/3) < \phi < \pi/2$ and $\pi + \arcsin(1/3) < \phi < 3\pi/2$. Therefore, the solutions are either $\phi = \pi - \alpha$ and $\phi = 2\pi - \alpha$ (third straight line through the positioning node) or $\phi = \beta$ and $\phi = \pi + \beta$ (fourth straight line through the positioning node).

For any of the situations mentioned above, the included angle between the two possible straight lines can be expressed as

$$\phi_{\text{inc}} = \alpha + \beta. \quad (9)$$

The value of ϕ_{inc} corresponding to the different real value of the azimuthal angle ϕ is shown in Fig. 2.

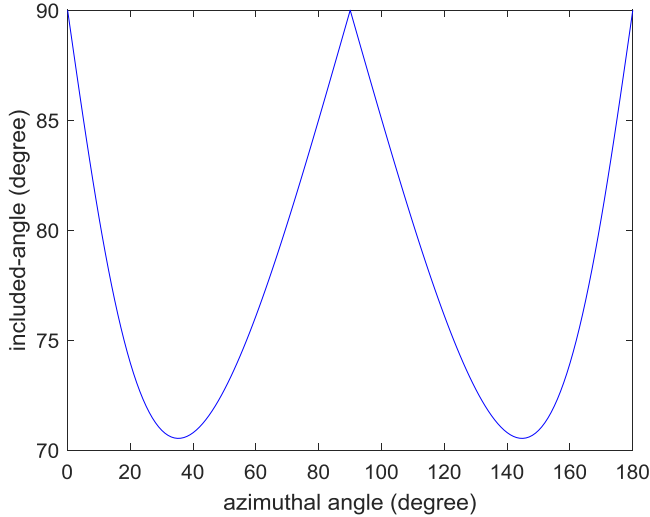


Fig. 2. Acute angle included between two possible straight lines.

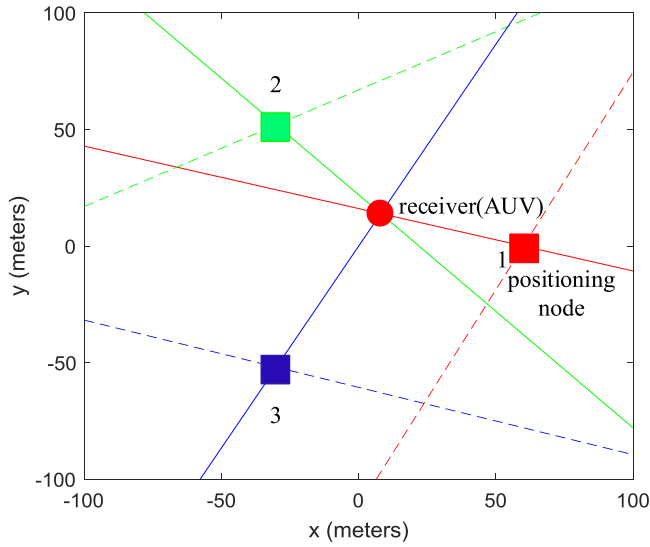


Fig. 3. Triangulating positioning with DOA.

It can be seen from Fig. 2 that the acute included angle between the two possible azimuthal positions is constrained. The value of the acute included angle is on the interval of [70.53, 90] (degrees).

C. Triangulating Positioning

Based on the estimated value of the azimuthal angle in the above analysis, the triangulating positioning can be achieved with DOA.

There are three positioning nodes located at the vertex points of a positive triangle, as shown in Fig. 3. Based on the measured data for E_x and E_y , χ can be obtained, and whether E_x and E_y are in-phase or not can be determined. Therefore, the two straight lines passing through each positioning node can be obtained according to (6), in conjunction with the above analysis, for the elimination of false solutions. The AUV is located on one of these two straight lines for each positioning node. Therefore,

the intersection of the three straight lines through the three positioning nodes is the actual position of the AUV. These three straight lines are shown with solid lines in Fig. 3. The other three dashed lines are the false solutions of (6).

For general positioning of the receiver inside the positive triangle, the above positioning process leads to a unique result for positioning. Because the acute included angle between two possible straight lines through each positioning node is greater than 60°, there is a unique intersection inside the positive triangle.

In Fig. 3, the side length of the positive triangle is 60 m. The azimuthal angles of the receiver relative to the three positioning nodes are 165°, 315°, and 60°.

III. POSITIONING ERROR CAUSED BY MEASUREMENT

The measurement error may be included in the parameter χ , thereby causing positioning error. The measured data can be described as

$$E'_x = E_x + \Delta E_x = (1 + \delta_x) E_x \quad (10)$$

$$E'_y = E_y + \Delta E_y = (1 + \delta_y) E_y. \quad (11)$$

The error for the azimuthal angle is then

$$\Delta\phi = \frac{d\phi}{d\chi} \left(\frac{\partial\chi}{\partial E_x} \Delta E_x + \frac{\partial\chi}{\partial E_y} \Delta E_y \right) \quad (12)$$

where

$$\frac{\partial\chi}{\partial E_x} = 2 \frac{E_x E_y^2}{(E_x^2 + E_y^2)^2} \quad (13)$$

$$\frac{\partial\chi}{\partial E_y} = - \frac{E_y E_x^2}{(E_x^2 + E_y^2)^2} \quad (14)$$

$$\frac{d\phi}{d\chi} = \pm \frac{1}{12 \cos \phi \sin \phi} \left(1 \pm \frac{\chi + 4}{\sqrt{\chi^2 + 8\chi}} \right). \quad (15)$$

It is assumed that ΔE_x and ΔE_y are independent of each other and satisfy the Gaussian distributions. Therefore, $\Delta\phi$ also satisfies a Gaussian distribution. The variance of $\Delta\phi$ can be expressed as

$$D(\Delta\phi) = \left| \frac{d\phi}{d\chi} \frac{\partial\chi}{\partial E_x} \right|^2 D(\Delta E_x) + \left| \frac{d\phi}{d\chi} \frac{\partial\chi}{\partial E_y} \right|^2 D(\Delta E_y). \quad (16)$$

Substituting (10) and (11) into (16), it can be obtained that

$$D(\Delta\phi) = \left| E_x \frac{d\phi}{d\chi} \frac{\partial\chi}{\partial E_x} \right|^2 D(\delta_x) + \left| E_y \frac{d\phi}{d\chi} \frac{\partial\chi}{\partial E_y} \right|^2 D(\delta_y). \quad (17)$$

Substituting (13)–(15) into (17), the root mean square (RMS) of the locating error of the azimuthal angle is

$$\xi(\Delta\phi) = Q \sqrt{D(\delta_x) + D(\delta_y)} \quad (18)$$

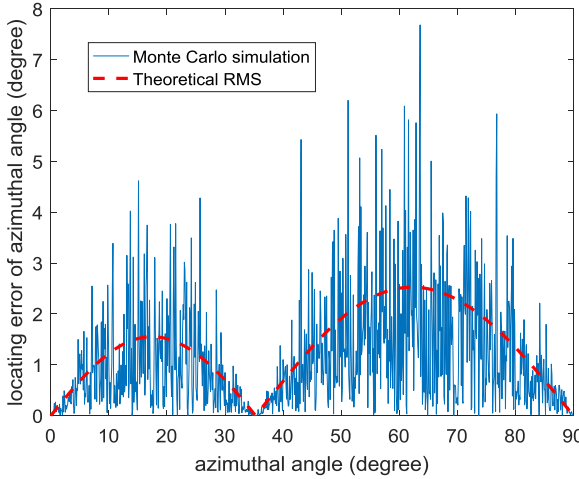


Fig. 4. Locating error for different azimuthal angle.

where

$$Q = \frac{3A^3}{2} \left(1 \pm \frac{\chi + 4}{\sqrt{\chi^2 + 8\chi}} \right) |(1 - 3 \sin^2 \phi) \sin \phi \cos \phi| \times \left| \frac{E_x}{(E_x^2 + E_y^2)^2} \right| \quad (19)$$

$$A = \left| \frac{Ids}{2\pi(\sigma - j\epsilon\omega)\rho^3} e^{\gamma(h-z)} \right|. \quad (20)$$

The \pm sign within the first parentheses [in (19)] is determined by the value of $(1 - 3 \sin^2 \phi)$, where $+$ is for $(1 - 3 \sin^2 \phi) < 0$ and $-$ is for $(1 - 3 \sin^2 \phi) > 0$.

When $D(\delta_x) = D(\delta_y) = 0.01$, Fig. 4 shows the numerical results for the positioning error for different azimuthal angles. The solid line is the result based on a Monte Carlo simulation. The dashed line is the result of (18). The two results are in agreement with each other.

It can be seen that the RMS of the locating error is less than 3° when $D(\delta_x) = D(\delta_y) = 0.01$. There are three zero points in Fig. 4, corresponding to $(1 - 3 \sin^2 \phi) \sin \phi \cos \phi = 0$ in (19).

IV. POSITIONING ERROR CAUSED BY THE TILTED SEA SURFACE

In practice, there are fluctuations on the sea surface. The fluctuations may cause perturbations in the field. Since the frequency is extremely low, a sea wave with a long wavelength is considered here. It is assumed that the sea wavelength is much longer than the transmitting-receiving distance. The sea surface can then be regarded as a tilted plane for the transmitter and the receiver, as shown in Fig. 5, where the tilt angle is τ .

The field at the receiver can be expressed as

$$E'_x = \cos \tau (E_x \cos \tau + E_z \sin \tau) + \sin \tau (E_{zx} \cos \tau + E_{zz} \sin \tau) \quad (21)$$

$$E'_y = E_y \cos \tau + E_{zy} \sin \tau \quad (22)$$

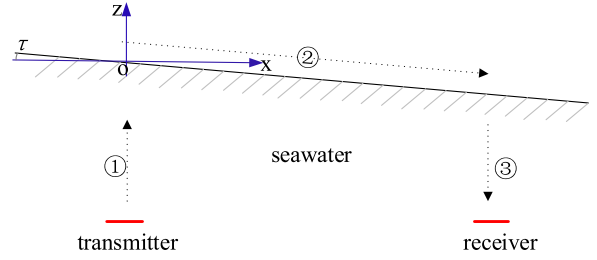


Fig. 5. Tilted sea surface.

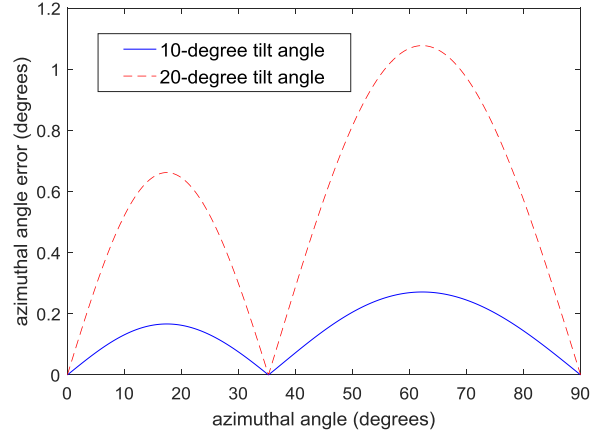


Fig. 6. Locating error for different azimuthal angles due to a tilt angle.

where E_{zx} , E_{zy} , and E_{zz} are the field components at the receiver when the transmitting dipole is vertical.

If $\tau \ll 1$, one can see that

$$E'_x \approx \cos^2 \tau E_x \quad (23)$$

$$E'_y \approx E_y \cos \tau. \quad (24)$$

Then

$$\chi' = \frac{\cos^4 \tau E_x^2}{\cos^4 \tau E_x^2 + \cos^2 \tau E_y^2} = \frac{\cos^2 \tau E_x^2}{\cos^2 \tau E_x^2 + E_y^2}. \quad (25)$$

Therefore, similar to (18), the error in the azimuthal angle, caused by the tilt angle, can be expressed as

$$\Delta\phi = Q (1 - \cos \tau). \quad (26)$$

The positioning error for different azimuthal angles is shown in Fig. 6 with tilt angles of 10° and 20° . It can be seen that the positioning error is less than 1.1° for a 20° tilt angle and less than 0.3° for a 10° tilt angle. The fluctuations on the sea surface seem to have a small influence on the positioning error with a low-frequency electromagnetic field.

V. CONCLUSION

It was demonstrated that the components of the near field in seawater can be used for positioning. The positioning error caused by the measurement error is related to the azimuthal position of the AUV. There are three zero points for the positioning error. The positioning error caused by the fluctuation of the sea surface is determined by the tilt angle of the sea surface for a long-wavelength sea wave.

REFERENCES

- [1] A. Sommerfeld, "Über die ausbreitung der wellen in der drahtlosen telegraphie," *Ann. Phys.*, vol. 28, pp. 665–736, 1909.
- [2] A. Banos Jr., *Dipole Radiation in the Presence of a Conducting Half-Space*. New York, NY, USA: Pergamon, 1966.
- [3] M. Dautta and Md. I. Hasan, "Underwater vehicle communication using electromagnetic fields in shallow seas," in *Proc. Int. Conf. Elect. Comput. Commun. Eng.*, Cox's Bazar, Bangladesh, Feb. 2017, pp. 38–43. doi: [10.1109/ECACE.2017.7912875](https://doi.org/10.1109/ECACE.2017.7912875).
- [4] P. Saini, R. P. Singh, and A. Sinha, "Path loss analysis of RF waves for underwater wireless sensor networks," in *Proc. Int. Conf. Comput. Commun. Technol. Smart Nation*, Gurgaon, India, Oct. 2017, pp. 104–108. doi: [10.1109/IC3TSN.2017.8284460](https://doi.org/10.1109/IC3TSN.2017.8284460).
- [5] R. W. P. King, "Dipoles in dissipative media," Crufit Lab., Harvard Univ., Cambridge, MA, USA, Tech. Rep. 336, Feb. 1961.
- [6] K. Iizuka and R. W. P. King, "The dipole antenna immersed in a homogeneous conducting medium," *IRE Trans. Antennas Propag.*, vol. AP-10, no. 4, pp. 384–392, Jul. 1962.
- [7] R. W. P. King, "Theory of the terminated insulated antenna in a conducting medium," *IEEE Trans. Antennas Propag.*, vol. AP-12, no. 3, pp. 305–318, May 1964.
- [8] R. K. Moore, "Theory of radio communication between submerged submarines," M.S. Thesis, Cornell Univ., Ithaca, NY, USA, Jun. 1951.
- [9] R. N. Ghose, "The radiator-to-medium coupling in an underground communication system," in *Proc. Nat. Conf. Electron.*, 1960, vol. 16.
- [10] C.-M. Tang, "Electromagnetic fields due to dipole antennas embedded in stratified anisotropic media," *IEEE Trans. Antennas Propag.*, vol. 27, no. 5, pp. 665–670, Sep. 1979.
- [11] J. A. Kong, "Electromagnetic fields due to dipole antennas over stratified anisotropic media," *Geophysics*, vol. 37, no. 6, pp. 985–996, 1972.
- [12] R. K. Moore, "Radio communication in the Sea," *IEEE Spectr.*, vol. 4, no. 11, pp. 42–51, Nov. 1967.
- [13] R. K. Moore and W. E. Blair, "Dipole radiation in a conducting half-space," *IEEE Trans. Antennas Propag.*, vol. 65D, no. 6, pp. 547–563, 1961.
- [14] M. Siegel and R. W. P. King, "Radiation from linear antennas in a dissipative half-space," *IEEE Trans. Antennas Propag.*, vol. AP-19, no. 4, pp. 477–485, Jul. 1971.
- [15] J. R. Wait, "The electromagnetic fields of a horizontal dipole in the presence of a conducting half-space," *Can. J. Phys.*, vol. 39, pp. 1017–1028, 1961.
- [16] H. Sato *et al.*, "Dipole antenna with sheath-cover for seawater use," in *Proc. Int. Symp. Antennas Propag.*, Phuket, Thailand, 2017, pp. 1–2. doi: [10.1109/ISANP.2017.8228941](https://doi.org/10.1109/ISANP.2017.8228941).
- [17] M. Siegel and R. W. P. King, "Electromagnetic propagation between antennas submerged in the Ocean," *IEEE Trans. Antennas Propag.*, vol. AP-21, no. 4, pp. 507–513, Jul. 1973.
- [18] M. B. Kraichman, "Basic experimental studies of the magnetic field from electromagnetic sources immersed in a semi-infinite conducting medium," *J. Res. Nat. Bur. Stand.*, vol. 64D, pp. 21–25, Jan./Feb. 1960.
- [19] A. I. Al-Shamma'a, A. Shaw, and S. Saman, "Propagation of electromagnetic waves at MHz frequencies through seawater," *IEEE Trans. Antennas Propag.*, vol. 52, no. 11, pp. 2843–2849, Nov. 2004.
- [20] H. Yoshida *et al.*, "Underwater LF wave propagation study for positioning," in *Proc. Int. Conf. OCEANS Aberdeen*, 2017, pp. 1–5. doi: [10.1109/OCEANSE.2017.8084829](https://doi.org/10.1109/OCEANSE.2017.8084829).
- [21] D. Arumugam, "Decoupled range and orientation sensing in long-range magnetoquasistatic positioning," *IEEE Antennas Wireless Propag. Lett.*, vol. 14, pp. 654–657, 2015. doi: [10.1109/LAWP.2014.2375873](https://doi.org/10.1109/LAWP.2014.2375873).
- [22] D. Arumugam, "Through-the-wall magnetoquasistatic ranging," *IEEE Antennas Wireless Propag. Lett.*, vol. 16, pp. 1439–1442, 2017. doi: [10.1109/LAWP.2016.2641421](https://doi.org/10.1109/LAWP.2016.2641421).